Safe Storage Parameters During CO_2 Injection Using Coupled Reservoir-Geomechanical Analysis

Tore Ingvald Bjørnarå*, Eyvind Aker, and Elin Skurtveit
NGI, PO Box 3930 Ullevål Stadion, Sognsveien 72, 0806 Oslo, Norway
*Corresponding author: tore.ingvald.bjornara@ngi.no

Abstract: Safe short term storage of CO_2 depends mainly on structural trapping; migration of injected CO_2 is blocked by impermeable cap rock, and solubility trapping; CO_2 dissolves in pore water. On longer term, mineral trapping is also contributing to the trapping of CO_2.

To be able to investigate the importance of these different storage mechanisms, a finite element model for simulation of CO_2 injection has been developed in COMSOL Multiphysics. The model describes and solves for two-phase flow (including dissolution of CO_2 in water) and fully coupled two-way interaction between the fluid flow and the solid displacement using elastic linear Biot poroelasticity theory.

A rudimentary model is presented here to illustrate the practical use of the model by determining the flow regime (considering dissolution of CO_2) and the stress distribution due to CO_2 injection into a formation.

The most important mechanisms for CO_2 storage seems to be residual and solubility trapping. Good storage conditions can be reservoirs with high air entry pressure values, since this tends to diffuse the CO_2 phase very efficiently.

Keywords: Two-phase flow, poroelasticity, porous media, CO_2

1. Introduction

Almost all produced hydrocarbon is, and will be, used as fuel and therefore produce CO_2 that eventually will be released into the atmosphere. In this perspective, plans for long-term storage of CO_2 are a good and sustainable idea for reducing climate effect of the atmospheric emission of CO_2. One of the most promising ideas is injecting CO_2 into a reservoir where it is stored indefinitely. Good potential geological formations to store captured CO_2 are depleted and disused oil and gas fields, deep saline aquifers and unminable coal seams [#1].

One ideal scenario is to inject CO_2 into a permeable aquifer underneath a very low-permeable caprock. When injected, CO_2 will dissolve in the reservoir water, increasing the density. After hundreds to thousands of years the injected CO_2 will react to form carbonates and precipitate and this is the safest storage mechanism. However, migration of the CO_2 beyond the natural reservoir seals could become problematic. Thus, modelling of CO_2 injection can help to better understand cause of leakage and its mechanisms and make CO_2 storage safer.

The trapping contributions of the various storage mechanisms as function of time is indicated in figure 1.

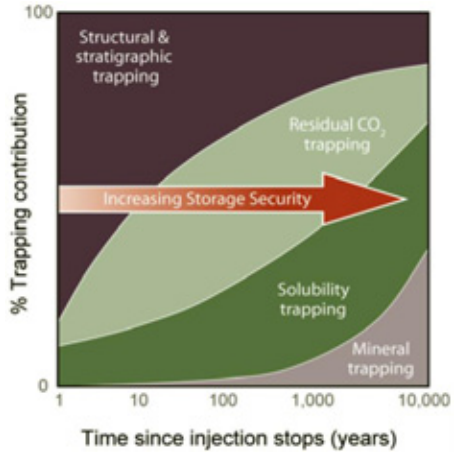

Figure 1. The trapping contributions of the various mechanisms as function of time. (Illustration from the IPPC Special report, 2005).

Storage of CO_2 depends mainly on the four trapping mechanisms (illustrated in figure 1):

1. Structural trapping; migration of injected CO_2 is blocked by impermeable cap rock
2. Residual trapping; capillary forces and adsorption onto the surfaces of mineral grains within the rock matrix immobilize (residual) parts of the injected CO_2
3. Solubility trapping; CO_2 dissolves and become trapped in the pore water. Dissolving CO_2 in water increases the density; hence the water with CO_2 will descend
4. Mineral trapping; Dissolved CO_2 forms carbonic acid, in time the surrounding

mineral dissolves and reacts with the CO_2 to form solid carbonates.

The timescales on which these processes operate need to be taken into account in CO_2 storage capacity assessment. Mineral trapping reactions that induce carbonate precipitation will play little part in creating additional space during CO_2 injection because they act too slowly. The kinetics of mineral trapping is so slow that they will only have a significant effect over hundreds to thousands of years. In practice, mineral trapping commonly can be ignored as a significant storage mechanism on a hundred-year timescale. To be able to investigate the importance of the other storage mechanisms a finite element model for simulation of CO_2 injection will be defined. The model describes and solves for two-phase flow (including dissolution of CO_2 in water) and fully coupled two-way interaction between the fluid flow and the solid displacement using elastic linear Biot poroelasticity theory.

2. Use of COMSOL Multiphysics

The system equations consists of two mass balances; one for each phase in the two-phase flow system, a mass balance for the dissolved CO_2 in water and a stress-strain application mode for modeling the geo-mechanics. The mass balances are all defined in PDE general form application mode.

3. Equations

In the following section, the various systems of partial differential equations that define the model are described.

3.1. Equations; two-phase flow

The two-phase flow formulation used in this paper is often referred to as fractional flow formulation. The background for the two-phase flow equations are the general mass balance equations. This approach treats the two-phase flow problem as a total fluid flow of a single mixed fluid, and then describes the individual phases as fractions of the total flow.

The general mass balance equation is defined as:

$$\frac{\partial(\phi\rho_\alpha S_\alpha)}{\partial t} + \nabla(\rho_\alpha \mathbf{u}_\alpha) = \rho_\alpha q_\alpha \qquad \text{Eq. 1}$$

In addition, auxiliary equations apply:

$$S_w + S_n = 1 \qquad \text{Eq. 2}$$

$$p_c(S_w) = p_n - p_w \qquad \text{Eq. 3}$$

The Darcy velocity is defined as:

$$\mathbf{u}_\alpha = -\frac{k_{r\alpha}}{\mu_\alpha}\mathbf{K}(\nabla p_\alpha - \rho_\alpha \mathbf{g}) \qquad \text{Eq. 4}$$

Doing some equation manipulations on equations 1-4 (for both wetting and non-wetting phase) results in an equation for the global pressure (total pressure) and an equation for the saturation of one of the phases (here for the wetting phase; S_w).

Note: There are many variations of the capillary pressure function and relative permeabilities, they can be expressed by for instance Van Genuchten or Brooks-Corey, in the Example model Van Genuchten is used, see appendix B for the expressions.

3.2 Equations; Biot linear poroelasticity

Linear Biot poroelasticity theory is used to account for elastic response of fluid saturated porous solid. The formulation is restricted to linear elastic solids undergoing quasistatic small deformations and is here based on Naviers equation for the study of displacements, stresses, and strains in an in-plane, or axial symmetric, loaded body. The formulation can also account for thermal strain using a thermal expansion coefficient.

Similar to thermal expansion, where change in temperature relative to a reference temperature can cause a solid to deform, poroelasticity combines the theory of fluid flow with constitutive equations that couple the stress in the porous solid and pore pressure due to fluid flow. An increase in fluid pressure will cause the porous solid to swell.

For more information on the theory background of small, linear and elastic deformations the reader is referred to Structural Mechanics Module User's guide manual in COMSOL Multiphysics [#2].

The equation for linear Biot poroelasticity:

$$\nabla \cdot [\boldsymbol{\sigma}] = -\mathbf{F} \quad \text{Eq. 5}$$

$$\boldsymbol{\sigma} = \mathbf{D}_{el}\varepsilon - \alpha_{biot} p\mathbf{I} \quad \text{Eq. 6}$$

The coupling between geomechanics and flow is: Deformation of a porous media affects the porosity:

$$\phi^* = (1-\varepsilon_v)\phi \quad \text{Eq. 7}$$

Additional source/sink terms to the mass balances (eq. 1) due to deformation:

$$q_w = q_n = -\alpha_{biot}\frac{\partial \varepsilon_v}{\partial t} \quad \text{Eq. 8}$$

Permeability is affected by porosity change according to [#3]:

$$K = K_0\left(\frac{\phi^*}{\phi}\right)^{20} \quad \text{Eq. 9}$$

(The exponent in eq. 9 can vary from case to case)

3.3 Equations; CO_2 mass balance

The chemical-part is implemented as strictly dissolution of super-critical (liquid) CO_2 in reservoir water. CO_2 solubility in water depends on pressure, temperature and salinity of the system. With the constant temperature profile, constant zero salinity of the water and the hydrostatic pressure used in the model, the saturation concentration of CO_2 in water varies very little and is therefore considered constant in the model [#4]. For a more detailed model, though, density variations in the water should be taken into consideration.

The general mass balance for the dissolved amount of CO_2 in water is given by:

$$\frac{\partial(\phi S_w C_{CO_2})}{\partial t} + \nabla \cdot (-D_{CO_2}\phi S_w \nabla C_{CO_2}) = F \quad \text{Eq. 10}$$

The natural source term F is defined as the dissolution T_d, described below.

Assuming that the dissolution of CO_2 in water is mass transfer controlled, a mass balance for the dissolved CO_2 in water is added to the system of equations. Dissolution of CO_2 in water is almost instantaneous is implemented as a sink in the non-wetting phase mass balance equation source term. Since CO_2 is miscible with water, it is not implemented as a source term to the wetting phase mass balance. The sink is defined as:

$$T_d = k_s(min(C_{sat,CO_2}S_w, C_{0,CO_2}S_n) - C_{CO_2}) \quad \text{Eq. 11}$$

Dissolution rate k_s of CO_2 in water is considered almost instantaneous. The value is unknown, here a rate of $0.5 \cdot 10^{-4}$ [s^{-1}] is used and meaning that after approximately ~5.6 hours dissolution of CO_2 in water has reached equilibrium.

Dissolved CO_2 and water is miscible and therefore has the same volume fraction as water, here the wetting phase; S_w.

min in eq. 11 is a function returning the minimum value of the two input arguments. This makes sure that dissolved CO_2 can never be more than available CO_2 in the non-wetting phase (liquid CO_2) or maximum saturation concentration of CO_2 in the wetting phase.

3.4 Equations; calculating *pH*

When the concentration of dissolved CO_2 in water is calculated, the *pH* can be evaluated. CO_2 dissolves in water according to the following equilibrium reactions:

I $CO_2(sc) \rightleftharpoons CO_2(aq)$
II $CO_2(aq) + H_2O(l) \rightleftharpoons H_2CO_3(aq)$

Treating $CO_2(aq)$ and $H_2CO_3(aq)$ as one entity, CO_2*:

III $CO_2^* + H_2O \rightleftharpoons HCO_3^-(aq) + H_3O^+(aq)$
IV $HCO_3^-(aq) \rightleftharpoons CO_3^{2-}(aq) + H_3O^+(aq)$

Using the protolysis constants from III and IV, K_{a1} and K_{a2}, respectively, the steuchiometric relation for initial concentration of carbonic acid, the water constant, K_w and applying electro neutrality, an expression for the *pH* is approximated to:

$$pH = -\log_{10}(\sqrt{K_{a1}C_{CO_2} + K_{a2}C_{CO_2} + K_w}) \quad \text{Eq. 12}$$

For the details of this derivation and values for the various constants K_w, K_{a1} and K_{a2}, see appropriate section in appendices. In real life, the pore water will have certain salinity and these constants can also depend on the salinity. Also, carbonates can act as buffers on the *pH* so in a more realistic model, more mass balances needs to be considered in order to get the "real" value, or more correct value, of the *pH*.

4. Model example; geometry

The geometry of the model is given in figure 2. It is a 300x300 m^2 domain consisting of a sand reservoir with a high permeability and porosity and two shale lenses with lower permeability and porosity, see table 1. The model is solved axial symmetric so the real size of the reservoir is 600x300 m^2.

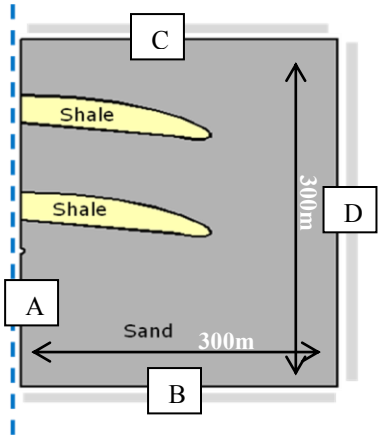

Figure 2. Illustration of geometry used in the model, note that the figure is not to scale. See text for explanation of boundary conditions.

Table 1. Material properties used in model, refer to figure 2.

	ϕ [-]	$\mathbf{K}_0$ [D]	p_d [kPa]	**E** [GPa]	ν [-]
Sand	0.4	3	20	2	0.3
Shale	0.1	0.01	20	2	0.3

Boundary A (blue dashed line in figure 2) is the axial symmetry line. The model domain is located 900 meters below the surface between two impermeable rocks; below (boundary B) and above (boundary C). To the right (boundary D) a fixed boundary condition is used for the global pressure p, saturation S_w.

Boundary A is constrained to move in the horizontal direction because of axial symmetry conditions, boundary B is constrained from moving at all, boundary D can move vertically only and boundary C is free to move.

Injection point is located in the centre of the domain, 170 meters below the top boundary, on the axial symmetry line A. The injection rate is equivalent to 30 kg/s (app. 1 mill ton/year) CO_2 being injected, and consists of 30 % water and 70 % CO_2. Dissolved CO_2 is assumed to be in equilibrium at the injection point.

5. Model example: results and discussion

Following are some discussions on the contributions of the various storage mechanisms.

5.1 Structural trapping

Migration of injected CO_2 is blocked by impermeable cap rock, if the permeability is low enough (close to impermeable), the fluid will not penetrate.

5.2 Residual trapping

Capillary forces and adsorption onto the surfaces of mineral grains within the rock matrix immobilize (residual) parts of the injected CO_2.

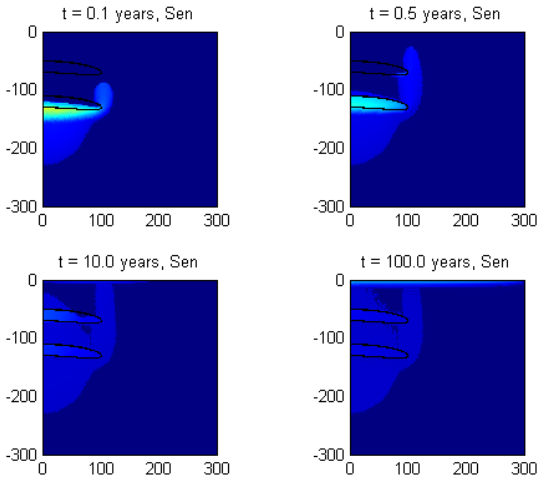

Figure 3. Residual trapping. The figure shows the non-wetting saturation (CO_2) for various times (from top left to lower right); 0.1, 0.5, 100 and 100 years. The plot shows how the injected CO_2 continue to rise, leaving a trail of undissolved CO_2 (equaivalent to a residual saturation of 5%).

In this case the injection of CO_2 into the reservoir is stopped after 0.1 year. CO_2 is lighter than water and will continue to rise. When the saturation of CO_2 reaches the saturation level, here defined at 5%, the effective non-wetting saturation and the Van Genuchten relative permeability approaches zero, hence immobilizing and stabilizing the CO_2.

5.3 Solubility trapping

CO_2 dissolves and become trapped in the pore water.

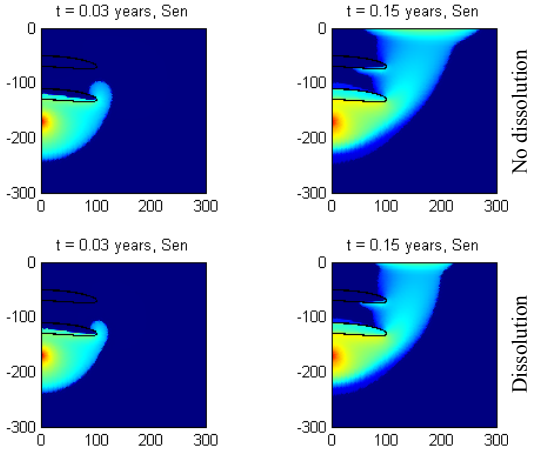

Figure 4. Solubility trapping. The colours show the saturation of non-wetting phase (here CO_2). The columns show the spreading of CO_2 phase for two times; 0.03 years and 0.15 years after injection. When including dissolution of CO_2 in water it is observed that some of the injected CO_2 is dissolved and trapped in the wetting (water) phase, slightly retarding the movement of the front of intruding CO_2.

Two models were solved; one where dissolution of CO_2 in water was taken into account and one where it was not taken into account. Comparing the two solutions show how CO_2 is dissolved and stabilized in the water; the CO_2 injection front moves slightly slower, see figure 4.

5.4 *pH*

Using equation 12, the *pH* can be evaluated in the model. In Figure 5 the *pH* is shown after two time steps: 0.03 and 0.1 years of injection. The *pH*-front follows exactly the CO_2 front (compare with figure 4).

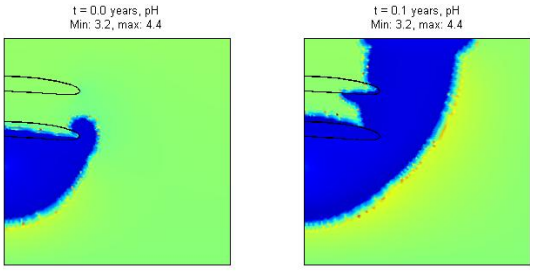

Figure 5. *pH* value in the reservoir after 0.03 years and 0.1 years of injection. The green color is approximately 4.4 and the blue color is app. 3.2.

5.5 Deformation

The increased pressure due to injection of CO_2 causes the reservoir to deform. Figure 6 shows a time series of the deformation due to injection.

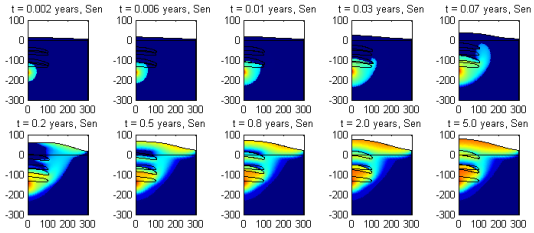

Figure 6. Deformation at various times; here exaggerated 5000 times.

In figure 7 deformations in selected points in the model is shown. The results show that the maximum deformation is achieved directly, on boundary C in figure 2 and is app. 14 mm.

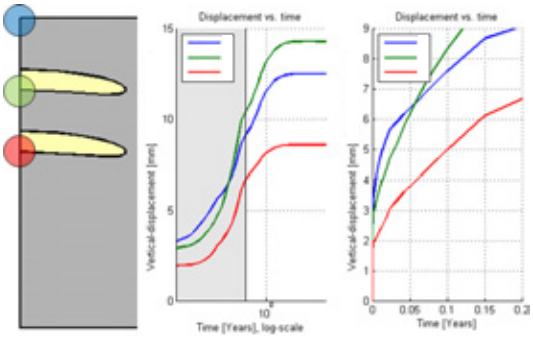

Figure 7. Deformation in selected points (indicated with the colors blue, green and red in the left figure) of the reservoir due to injection of CO_2. A close-up of the shaded area in the middle figure is given in the right figure.

6. Conclusion

A robust model for CO_2 storage and injection modelling, considering two-phase flow, simple chemistry considering dissolution of CO_2 in water and linear elastic poroelasticity has been developed using COMSOL Multiphysics.

The most important mechanisms for CO_2 storage seems to be residual and solubility trapping. Good storage conditions can be reservoirs with high air entry pressure values, since this tends to diffuse the CO_2 phase very efficiently.

The large variations in *pH* indicate that *pH* measurements can be a very good detection method in monitoring.

Proper boundary conditions need more attention. It can be seen at longer times that the right boundary affects the dissolved CO_2 concentration, extracting the non-wetting phase and thereby lowering the concentration and increasing the *pH*.

To make the model more complete, more advanced material models for the soil can be used and/or implemented. Also, more chemical reactions can be added to more accurate description of the spreading of CO_2 and *pH* calculation.

Geomechanical modelling can in general say something about cause of fracturing, faulting and induced brittle deformation. This can be done using failure criteria such as the Drucker-Prager, the Lade, and the Coulomb failure criteria. These criteria provide different relationship between rock failure and the principal stresses, but no failure criterion is evaluated in this study. Also, brittle failure criteria can estimate slip tendency of faults and estimate maximum fluid pressure that can be attained during injection.

7. References

1. Chadwick, Andy; Arts, Rob; Bernstone, Christian; May, Franz; Thibeau, Sylvain; Zweigel, Peter, 2008, *"Best Practice for the Storage of CO_2 in Saline Aquifers - Observations and Guidelines from the SACS and CO2STORE projects"*. Nottingham, UK, British Geological Survey, 267pp. (British Geological Survey Occasional Publication, 14).
2. COMSOL Multiphysics User manual, Structural Mechanics Module, v.3.5a
3. Piri, Mohammad, Prévost, Jean H., Fuller, Richard, *"Carbon Dioxide Sequestration in Saline Aquifers: Evaporation, Precipitation and Compressibility Effects"*, presented at the FOURTH ANNUAL CONFERENCE ON CARBON CAPTURE AND SEQUESTRATION DOE/NETL, May 2-5, 2005
4. Diamond, Larryn W., Akinfiev, Nikolay N., *"Solubility of CO_2 in water from −1.5 to 100 C and from 0.1 to 100 MPa: evaluation of literature data and thermodynamic modeling"*, Fluid Phase Equilibria 208 (2003) 265–290
5. Morel-Seytoux, Hubert J., Philip D. Meyer, Mahmood Nachabe, Jaoudat Touma, M. T. Van Genuchten and Robert J. Lenhard, *"Parameter equivalence for the Brooks-Corey and Van Genuchten soil characteristics: Preserving the effective capillary drive"*, Water Resources Research, vol. 32, No. 5, p. 1251-1258, may 1996

8. Acknowledgements

Acknowledgements: Financial support from the Research Council of Norway and NGI is gratefully acknowledged

Appendix A. Nomenclature

Table 1: Symbols used in this paper

ϕ	Effective reservoir porosity, [-]
ϕ^*	Intrinsic reservoir porosity, [-]
ρ_α	Density, [kg/m^3]
α	Phase index, α can be w - wetting phase, or n - non-wetting phase, [-]
S_α	Saturation, [-]
$S_{e\alpha}$	Effective saturation for phase α, [-]
S_{wr}	Residual wetting sat. phase, [-]
S_{nr}	Residual non-wetting sat. phase, [-]
t	Time, [s]
p_c	Capillary pressure function, from Van Genuchten relations, [Pa]
p_α	Partial pressure, [Pa]
q_α	Source term, [m^3/s]
$k_{r\alpha}$	Relative permeability coefficient, from Van Genuchten relations, [-]
μ_α	dynamic viscosity, [kg/ms]
p	Global fluid pressure, [Pa]
$\mathbf{K}_0$	Intrinsic permeability tensor, [m^2]
$\mathbf{K}$	Effective permeability tensor, [m^2]
$\mathbf{g}$	Gravity coefficient vector, [m/s^2]
$\boldsymbol{\sigma}$	Stress tensor, [Pa]
$\mathbf{F}$	Body force vector, [N]
$\mathbf{D}_{el}$	Elasticity matrix, [Pa]
$\mathbf{E}$	Youngs modulus, [Pa]
v	Poisson ratio, [-]
$\boldsymbol{\varepsilon}_{el}$	Elastic strain, [m/m]
ε_v	Volumetric strain, [m/m]
α_{biot}	Biot coefficient, [-]
$\mathbf{I}$	Identity matrix, [-]
C_{CO2}	Concentration dissolved CO_2, [mol/m^3]
T_d	Dissolution rate CO_2, [mol/(m^{3}s)]
k_s	Mass transfer rate, [1/s]
$C_{sat,CO2}$	Saturation concentration CO_2, [mol/m^3]
$C_{0,CO2}$	Molar density of CO_2, [mol/m^3]
K_{a1}	Carbonic acid dissociation constant, first dissociation reaction, [-]
K_{a2}	Carbonic acid dissociation constant, second dissociation reaction, [-]
K_w	Water dissociation constant, [-]
m	Model parameter, [-]
n	Model parameter, [-]
p_d	Air entry pressure, [Pa]
λ,λ_α	Total mobility, mobility for phase α, [ms/kg]
f_α	Mobility fraction phase α, [-]

Appendix B. Van Genuchten relations

The advantage of using van Genuchten vs. Brooks-Corey functions is that the derivatives are continuous, improving numerical stability.

Capillary pressure vs. saturation function:

$$p_c(S_{ew}) = \frac{1}{\alpha}\left(S_{ew}^{-\frac{1}{m}} - 1\right)^{\frac{1}{n}} \quad \text{(B.1)}$$

The effective wetting saturation, S_{ew}, is given by:

$$S_{ew} = \frac{S_w - S_{wr}}{1 - S_{wr} - S_{nr}} \quad \text{(B.2)}$$

where $S_{ew} \in [0,1]$.

The derivative is analytically derived:

$$\frac{\partial p_c}{\partial S_{ew}} = -\frac{1}{\alpha}\cdot\frac{1}{n}\left(S_{ew}^{-\frac{1}{m}} - 1\right)^{-\frac{m-1}{m}} \cdot \frac{1}{m} S_{ew}^{-\frac{1+m}{m}} \quad \text{(B.3)}$$

Relative permeability functions to the van Genuchten model:

$$k_{rw}(S_{e\alpha}) = S_{e\alpha}^{\frac{1}{2}} \cdot \left(1 - \left(1 - S_{e\alpha}^{\frac{1}{m}}\right)^m\right)^2 \quad \text{(B.4)}$$

$$k_{rn}(S_{e\alpha}) = (1 - S_{e\alpha})^{\frac{1}{3}} \cdot \left(1 - S_{e\alpha}^{\frac{1}{m}}\right)^{2m} \quad \text{(B.5)}$$

Note: The relation between the air entry pressure and the fitting parameter α is given by [#5]:

$$\frac{1}{\alpha} = p_d \frac{2x(x-1)}{x+3}\frac{55.6 + 7.4x + x^2}{147.8 + 8.1x + 0.092x^2} \quad \text{(B.6)}$$

Where

$$x = 1 + 2/m \quad \text{(B.7)}$$

Appendix C. Velocity vectors

The velocity expressions for the two phases:

$$\mathbf{u}_w = f_w \mathbf{u} + \lambda_n f_w \mathbf{K}(\nabla p_c + (\rho_w - \rho_n)\mathbf{g}) \quad \text{(C.1)}$$

$$\mathbf{u}_n = f_n \mathbf{u} - \lambda_w f_n \mathbf{K}(\nabla p_c + (\rho_w + \rho_n)\mathbf{g}) \quad \text{(C.2)}$$

The total velocity expression:

$$\mathbf{u} = -\mathbf{K}(\lambda \nabla p - (\lambda_w \rho_w + \lambda_n \rho_n)\mathbf{g}) \quad \text{(C.3)}$$

Mobility (wetting/non-wetting phase/total)

$$\lambda_w = k_{rw}/\mu_w,\ \lambda_n = k_{rn}/\mu_n,\ \lambda = \lambda_w + \lambda_n \quad \text{(C.4-6)}$$

Mobility fraction (wetting/non-wetting):

$$f_w = \lambda_w/\lambda,\ f_n = \lambda_n/\lambda \quad \text{(C.7-8)}$$

Capillary pressure gradient:

$$\nabla p_c = \frac{\partial p_c}{\partial S_w}\nabla S_w \quad \text{(C.9)}$$